Grid Oscillators with Selective-Feedback Mirrors

Qi Sun, *Student Member, IEEE*, Jason B. Horiuchi, Steven R. Haynes, *Student Member, IEEE*, Kevin W. Miyashiro, *Student Member, IEEE*, and Wayne A. Shiroma, *Member, IEEE*

***Abstract*— Analytical and experimental results are presented that demonstrate the advantages of replacing the metal mirror of a C-band transistor-grid oscillator with two types of selective-feedback mirrors. The first mirror is a two-dimensional photonic crystal, whose frequency-, polarization-, and reflectivity-dependent characteristics result in higher radiated power, lower cross polarization, and improved locking. The second is a diode-loaded grating functioning as an electronically tunable mirror, which allows the oscillator to be amplitude-modulated.**

***Index Terms*—Photonic crystals, quasi-optical arrays.**

I. Introduction

A GRID OSCILLATOR consists of an array of solid-state devices loading a metal grating that is etched onto a dielectric substrate [1]. When properly designed, the grid radiates a linearly polarized wave whose power is the combined output of each device. Such quasi-optical power-combining schemes overcome the limited power-handling capability of semiconductor devices [2].

Among the most important figures-of-merit of a grid oscillator array are the oscillation frequency, power, directivity, harmonics, polarization, and noise. In practice, optimizing each of these characteristics simultaneously is difficult, since changing one design parameter (e.g., the unit-cell geometry, substrate permittivity, or mirror spacing) to improve one characteristic could adversely affect another one. Increasing the substrate thickness, for example, can lead to higher power, but can also result in the excitation of multiple modes [3]. Conversely, an electrically thin substrate can eliminate high sidelobes [4], but does not necessarily yield maximum power.

Part of the difficulty arises from the inherent design constraints associated with conventional grid-oscillator topologies, for example, in assuming that one must use a metal mirror. In this paper, the constraint of using a metal mirror with fixed reflectivity for all frequencies and polarizations is removed. Instead, the metal mirror is replaced with two different selective-feedback mirrors that are frequency-, polarization-, and reflectivity-dependent. Fig. 1 illustrates the idea with a photonic-crystal mirror and a tunable frequency-selective surface.

Both of these mirrors have the following selective-feedback properties that make them an attractive substitute for the metal reflector in a grid oscillator.

- *Frequency Dependence*: By designing the reflector to be frequency-dependent, only the desired mode in an otherwise multimoded grid builds up. This is important, for example, in pulsed operation, in which the oscillator should always turn on at the design frequency.
- *Polarization Dependence*: By designing the reflector to be polarization-dependent (reflecting only the vertical polarization back to the transistor array in Fig. 1), the cross polarization ratio can be improved.
- *Variable Reflectance*: Both of the alternative mirrors discussed here can be designed to have stopbands with sloping bandedges. By allowing the oscillator to operate along the edge of the stopband, the optimum feedback level for maximum power can be selected.

Section II discusses a technique for modeling grid oscillators with different mirrors. Results for a grid oscillator with a metal reflector, a photonic-crystal reflector, and an electronically tunable reflector are presented in Sections III–V, respectively.

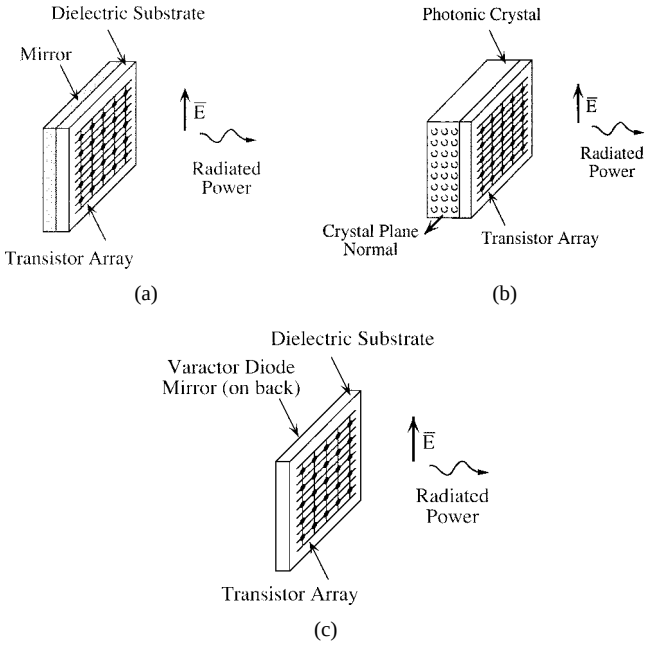

Fig. 1. A grid oscillator using a (a) metal reflector, (b) a photonic-crystal reflector, and (c) an electronically tunable reflector. For unidirectional radiation, an absorbing sheet can be placed on the backside in cases (b) and (c).

II. Modeling Approach

A grid oscillator can be modeled as the interconnection of two separate two-port networks, one representing the transistor and the other representing the embedding circuit, which consists of the metal grating, dielectric substrate, mirror, and free space. The embedding circuit is most often obtained from an analysis based on the unit-cell approximation [1], [5].

Manuscript received March 27, 1998; revised August 3, 1998. The work of J. Horiuchi was supported under a NASA Undergraduate Fellowship from the Space Grant College at the University of Hawaii at Manoa.

The authors are with the Department of Electrical Engineering, University of Hawaii at Manoa, Honolulu, HI, 96822 USA.

Publisher Item Identifier S 0018-9480(98)09201-1.

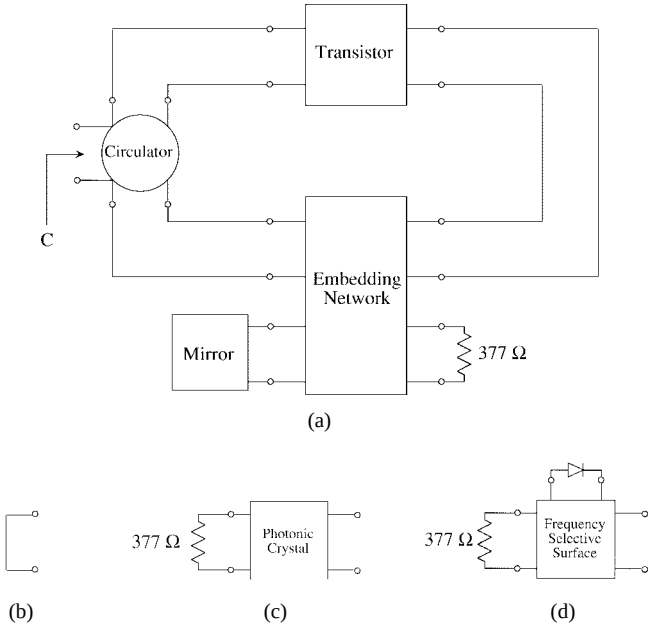

Fig. 2. (a) Equivalent circuit for analyzing grid oscillators, and the different types of mirrors analyzed. (b) Metal reflector. (c) Photonic-crystal reflector. (d) Electronically tunable reflector. Free space is modeled as a 377-Ω resistor. The circulator is used to determine the circular function C of the circuit.

A more flexible approach is discussed in [6], and later modified in [7] and [8], in which the embedding circuit is modeled as a four-port network that characterizes the metal grating and dielectric substrate alone. Two additional ports represent the free space in front and in back of the grid. Access to the free space allows for cascading of grids, or in this paper, the investigation of different types of mirrors, as shown in Fig. 2. A conventional metal reflector is modeled as a short circuit, a photonic-crystal reflector as a two-port network, and an electronically tunable reflector as a three-port network.

A loop-gain analysis determines whether the circuit satisfies the oscillator startup, steady-state, and maximum-power conditions at the design frequency. This can be conveniently carried out using circular-function [9] analysis on a microwave-circuit simulator. Circular-function analysis of an oscillator is summarized in Fig. 3. Plotted on the y-axis is the magnitude of the circular function when its phase is an integral multiple of 2π. If the circular function has a magnitude less than one, no oscillation is possible, as there is not enough positive feedback. The solid line indicates an optimum circular function at which the feedback level is set to yield maximum oscillator power [3]. If the oscillator has a circular function above this line, the power will be less than the maximum possible because the feedback level is too high. Below this line, the feedback level is too low.

To demonstrate how the type of mirror affects the feedback level, a proof-of-concept series of experiments was carried out using inexpensive, low-power transistors (HP-Avantek ATF-35576 pHEMT's). The optimum circular function for this transistor is shown in Fig. 4 as a solid line. A 5×5 grid oscillator was designed using a full-wave technique [5]. The period of the grid is 8 mm with 1-mm-wide bias lines and radiating leads, and is printed on a 2.54-mm-thick *Duroid* substrate with $\epsilon_r = 10.5$.

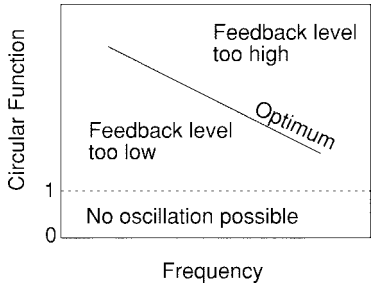

Fig. 3. The optimum circular function concept. The circular function is dependent on the S-parameters of the transistor and the embedding network, and for simplicity is shown here as a linear function of frequency.

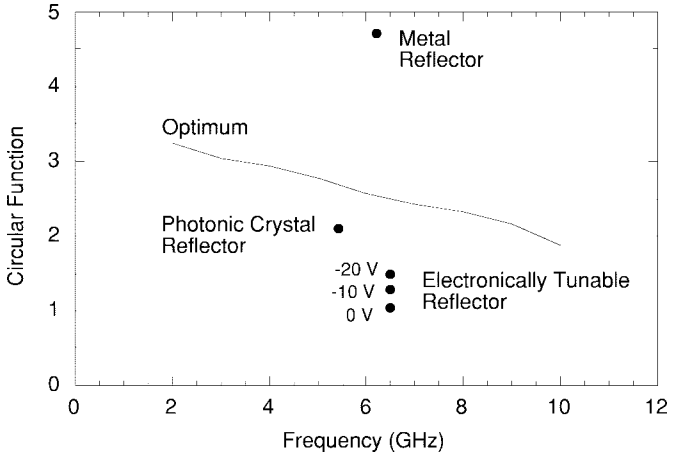

Fig. 4. Circular function versus frequency for the HP-Avantek ATF-35576 pHEMT. The optimum circular function is shown as a solid line. The dots represent grids with different types of mirrors discussed in the text.

III. Metal Reflector

With a metal reflector placed directly behind the substrate, the grid oscillates at 4.6 GHz with an equivalent isotropic radiated power (EIRP) of 0.07 W, a cross-polarization ratio of 11 dB and a second-harmonic level of -9 dBc. To improve the performance, a 12.7-mm-thick layer of *Stycast HiK* ($\epsilon_r = 10$) was inserted between the substrate and mirror. Increasing the substrate thickness had the effect shown in Fig. 5(a), in which the oscillator initially turns on with competing oscillation modes at 4.1 and 6.2 GHz, an effect which is also predicted by circular-function analysis, as shown in Fig. 5(b). The oscillator locks to the 6-GHz mode only after the gate bias is readjusted, yielding a higher EIRP of 0.20 W, a larger cross-polarization ratio of 18 dB, and a lower second-harmonic level of -20 dBc [Fig. 5(c)]. Despite this improved performance, Fig. 4 suggests that the feedback level is still too high.

IV. Photonic-Crystal Reflector

The results of Section III showed that for this particular transistor and unit-cell design, a thicker substrate allowed the oscillator to move closer to its optimum feedback level. However, this is also accompanied by the introduction of other potential oscillation modes. Changing the substrate thickness also results in a change in the oscillation frequency, making it necessary to redesign the unit-cell dimensions if a particular oscillation frequency is desired. To address these problems,

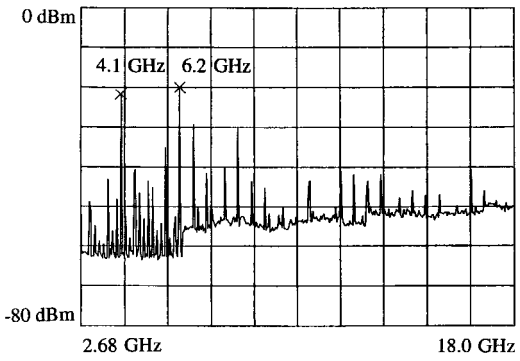

(a)

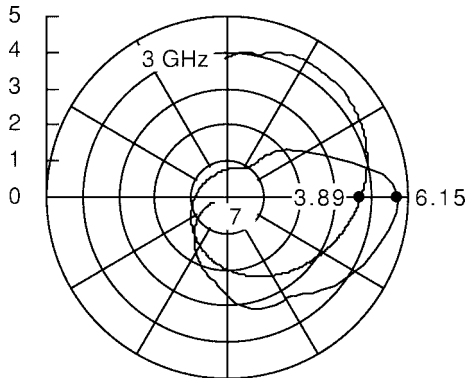

(b)

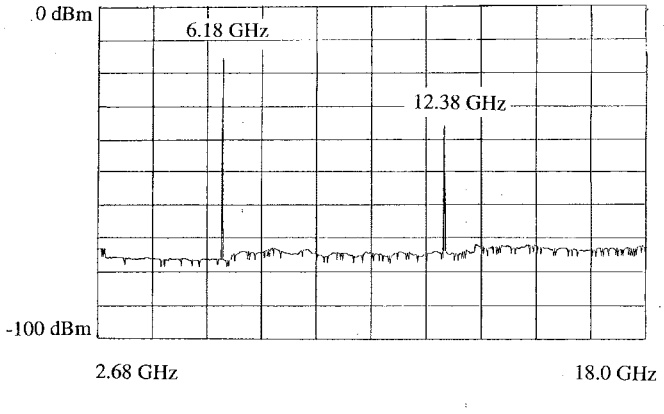

(c)

Fig. 5. Grid oscillator with a metal reflector showing (a) the measured spectrum when initially turned on, (b) the simulated circular function showing competing oscillation modes, and (c) the locked oscillator after the dc bias is adjusted.

the metal reflector was replaced with a photonic crystal (PC), while keeping the substrate thickness the same. The PC was also designed at a specific frequency to determine whether the grid could be forced to oscillate at that frequency.

A. Photonic Crystal Characteristics

A photonic crystal [10] is an artificial dielectric structure whose electromagnetic dispersion relation has a band structure similar to that of electrons in a crystalline solid. Stopbands and passbands in frequency arise from constructive interference in reflection or transmission, respectively. For the PC in Fig. 1(b) to replace the metal reflector in Fig. 1(a), it should have a stopband at the desired oscillation frequency.

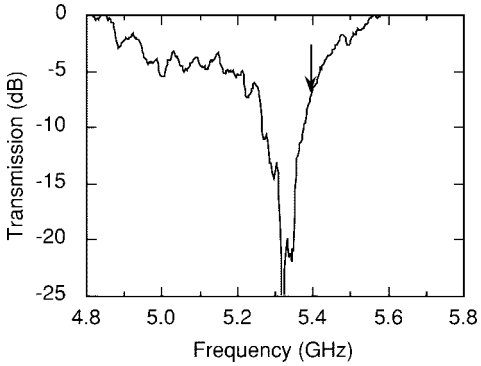

Fig. 6. Measured transmission characteristic of the photonic crystal. The arrow indicates the oscillation frequency of the grid at 5.4 GHz.

The PC was designed for a 4.7–5.8-GHz stopband using an atlas of two-dimensional PC's [11]. The PC topology consists of a square lattice of air columns (lattice constant $= 1.56$ cm, radius $= 0.59$ cm) in *Stycast HiK* ($\epsilon_r = 10$). The PC was specifically designed to have a transverse-electric (TE) stopband [11] to reflect only the copolar component of the oscillator, whose vertically polarized electric field is transverse to the crystal-plane normal of Fig. 1(b). The cross-polar component, whose electric field is parallel to the crystal-plane normal, would not be affected by the TE stopband. An absorbing sheet on the back of the PC terminates such undesired back-radiation.

The transmission characteristic of the PC was measured using a network analyzer and a pair of wideband horn antennas. Fig. 6 indicates a 25-dB transmission null at the design frequency. This null was nonexistent when both horns were rotated 90°, demonstrating that the stopband was indeed polarization-dependent.

B. Experimental Results

When the metal reflector was replaced with the PC, the unlocked spectrum of Fig. 5(a) was no longer observed. In fact, Fig. 7 shows that the oscillator immediately locks to 5.4 GHz (a frequency that is within the stopband of the crystal) upon applying the dc bias. This result compares favorably with the circular-function simulation shown in Fig. 8.

The fact that this single-mode oscillation occurs within the stopband of the PC has promising implications in the design process. Designing a grid is often an iterative process. To a large extent, the unit-cell size determines the oscillation frequency. Maximizing the power may dictate varying the substrate characteristics, but this also affects the oscillation frequency, requiring a readjustment of the unit-cell size. Several such iterations may be necessary to complete the design. Employing a PC-reflector offers greater flexibility by widening the design-parameter space. For example, if the PC stopband is designed to set the oscillation frequency, the unit-cell geometry and substrate characteristics can be left to address other issues, such as suppressing substrate modes [4], without affecting the frequency.

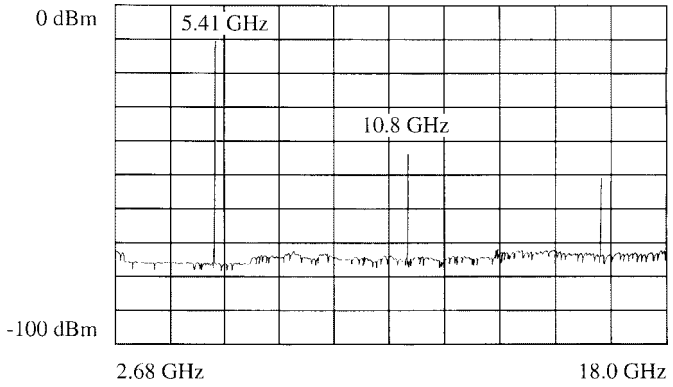

Fig. 7. Measured spectrum of the grid oscillator with a photonic-crystal reflector.

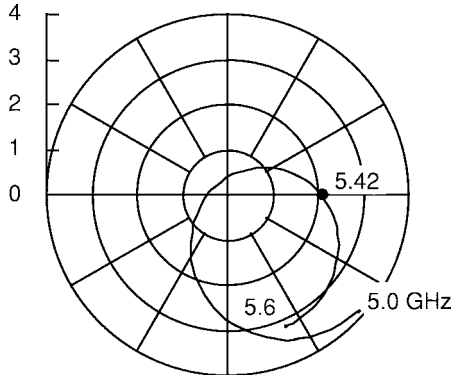

Fig. 8. Simulated circular function of a grid oscillator with a photonic-crystal reflector.

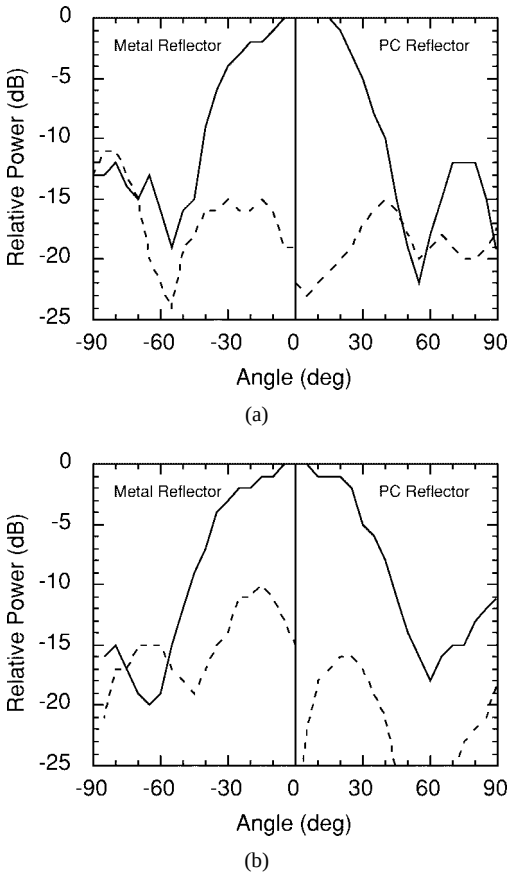

Fig. 9. Measured patterns of the grid oscillator with a metal versus photonic-crystal reflector. (a) H-plane. (b) E-plane. The solid line represents the copolarization, and the dashed line represents the cross polarization.

TABLE I
COMPARISON OF METAL VERSUS PC REFLECTOR

Reflector Type	Osc. Freq. (GHz)	EIRP (W)	Cross-pol Ratio (dB)	2nd Harmonic (dBc)
Metal	6.2	.20	18	-20
PC	5.4	.55	22	-32

Table I summarizes the results comparing the grid oscillator with a metal reflector versus a PC reflector. With the PC, the cross-polarization ratio at boresight increases by 4 dB, an improvement that we attribute to the polarization dependence of the crystal.

Fig. 9 compares the radiation patterns for the two cases. An estimate of the gain based on the 3-dB beamwidths reveals that it is nearly the same for both configurations. Since EIRP is the product of output power and gain, the fact that the EIRP for the PC case is higher than that of the metal-reflector case suggests that the grid oscillator with the PC is actually delivering higher output power. While it is true that the drain current for the PC-reflector case was 1.7 times higher than the metal-reflector case, this is not sufficient to explain the nearly three-fold increase in EIRP indicated in Table I.

The reason for the power increase can be explained from the theory in [3]. For the thickness of *Stycast* used in this experiment, circular-function analysis reveals that placing a metal reflector on the back of the *Stycast* yields a feedback level that is too high, resulting in a power level that is less than optimal. Replacing the metal reflector with a PC introduces a mechanism for reducing this feedback. Fig. 6 illustrates the idea. If the oscillation frequency lies in the center of the stopband, where the transmission is a minimum (and reflection is a maximum), then the power reflected back to the grid from the crystal may be too high, resulting in excessive gain compression of the transistors. However, if the oscillation frequency lies on the bandedge, as it does in Fig. 6, the feedback level is reduced, the devices are less compressed, and the output power increases. This is also seen in Fig. 4, where the circular function of the grid with a PC reflector is much closer to the optimum than the grid with a metal reflector.

V. ELECTRONICALLY TUNABLE REFLECTOR

In [12], a quasi-optical voltage-controlled oscillator is realized by placing a varactor-diode grid in the near field of a transistor grid, with a metal reflector located some distance away. By adjusting the dc bias of the diode grid, the transistor grid's oscillation frequency varies continuously over a 10% bandwidth.

This section discusses a different application of a cascaded pair of transistor and varactor-diode grids, in which the oscillator's power is electronically tuned while maintaining a constant frequency. As shown in Fig. 1(c), the metal reflector is replaced with a varactor grid, which serves as a variable-feedback mirror that provides amplitude modulation.

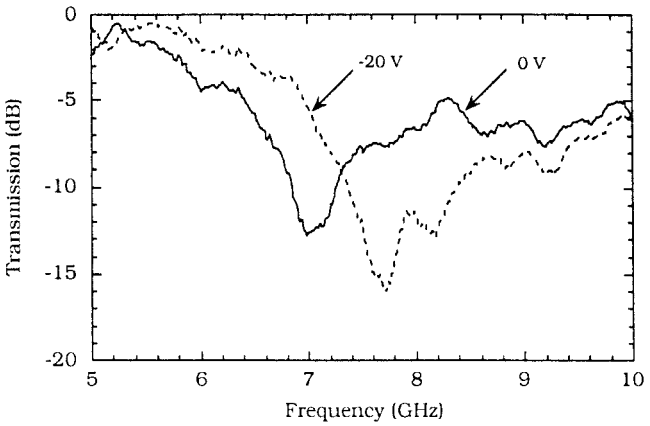

Fig. 10. Measured transmission characteristic of the varactor-loaded grid.

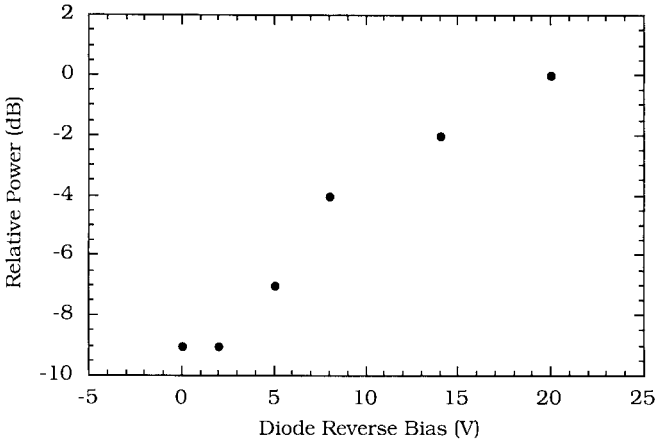

Fig. 11. Measured oscillator power as a function of reverse diode voltage. The oscillation frequency is constant at 7.13 GHz.

In contrast to the configuration in [12], the diode and transistor grids here are separated by an electrically thick substrate, so that frequency tuning is minimized.

A. Reflector Measurements and Modeling

A 5×5 diode grid was fabricated on 1.27-mm-thick *Duroid* with $\epsilon_r = 10.5$. The layout was identical to the transistor grid described in Section II, but with just two bias lines per row of devices instead of three. Metelics MSV-34 varactor diodes were loaded onto the grid. Free-space transmission measurements in Fig. 10 indicate that the resonant frequency of the grid could be electronically tuned over a 10% bandwidth. Another way of interpreting this plot is to say that the transmission (or reflection) can be electronically tuned at a fixed frequency. For example, dc-bias tuning provides a 7-dB transmission tuning range at 7 GHz.

Following the approach outlined in Section II, the diode grid is modeled as a three-port network as shown in Fig. 2(d). To simulate the free-space measurement described above, two of the ports are connected to 377-Ω resistors representing free space, and the remaining port connected to a diode model. For simplicity, capacitors of different values were used to simulate the dc-bias control of the diode junction capacitance. The values of the capacitors were chosen such that the simulated resonant frequencies matched the measured resonant frequencies of Fig. 10.

B. Amplitude Modulation

Once the capacitor values corresponding to diode voltage were selected, a circular-function analysis was performed for the circuit of Fig. 2(a), with the three-port network of the diode grid serving as the mirror. As the capacitance value was decreased, simulating an increase in the reverse diode voltage, the oscillation frequency varied from 6.48 to 6.50 GHz, a difference of less than 1%. However, the magnitude of the circular function varied from 1.0 to 1.5. From Fig. 4, we note that increasing the reverse diode voltage has the simulated effect of increasing the feedback toward the optimum level. Therefore, we should expect the power to increase with reverse voltage, with a negligible change in frequency.

This is exactly the situation that was observed experimentally. With the varactor diodes biased at 0 V, the oscillator locked at 7.13 GHz, which is near the resonant frequency of the diode grid (Fig. 10). The reverse bias voltage was then increased, and the oscillator EIRP was observed to steadily increase (Fig. 11). The oscillation frequency for all bias points remained within 1% of 7.13 GHz, but the power changed by nearly 10 dB.

This demonstrates how amplitude modulation could be conveniently implemented in a grid oscillator. Instead of applying the modulating signal through the dc bias of the transistor grid, which is often so sensitive to bias as to occasionally unlock [Fig. 5(a)], the modulation could be applied as a control signal to the mirror. The carrier frequency remains constant, but the amplitude varies as a function of the mirror's feedback.

VI. Conclusion

Replacing the metal reflector with a selective-feedback reflector was shown to improve the performance and simplify the design of grid-oscillator arrays. Using a photonic-crystal reflector resulted in higher radiated power, lower cross polarization, reduced harmonic content, and improved locking. Using a varactor-diode reflector resulted in electronic power control with negligible change in frequency.

References

[1] Z. B. Popović, R. M. Weikle II, M. Kim, and D. B. Rutledge, "A 100-MESFET planar grid oscillator," *IEEE Trans. Microwave Theory Tech.*, vol. 39, pp. 193–200, Feb. 1991.

[2] J. W. Mink, "Quasi-optical power combining of solid-state millimeter-wave sources," *IEEE Trans. Microwave Theory Tech.*, vol. MTT-34, pp. 273–279, Feb. 1986.

[3] W. A. Shiroma and Z. Popović, "Analysis and optimization of grid oscillators," *IEEE Trans. Microwave Theory Tech.*, vol. 45, pp. 2380–2386, Dec. 1997.

[4] P. Preventza, M. Matloubian, and D. B. Rutledge, "A 43-GHz AlInAs/GaInAs/InP HEMT grid oscillator," in *1997 IEEE MTT-S Int. Microwave Symp. Dig.*, Denver, CO, June 1997, pp. 1057–1060.

[5] S. C. Bundy and Z. B. Popović, "A generalized analysis for grid oscillator design," *IEEE Trans. Microwave Theory Tech.*, vol. 42, pp. 2486–2491, Dec. 1994.

[6] W. A. Shiroma, S. C. Bundy, S. Hollung, B. D. Bauernfeind, and Z. B. Popović, "Cascaded active and passive quasi-optical grids," *IEEE Trans. Microwave Theory Tech.*, vol. 43, pp. 2904–2909, Dec. 1995.

[7] W. A. Shiroma, "Cascaded active and passive grids for quasi-optical front ends," Ph.D. dissertation, Univ. of Colorado, Boulder, CO, 1996.
[8] J. W. Dixon, "Linear and nonlinear modeling of quasi-optical oscillators and amplifiers," Ph.D. dissertation, Univ. of Colorado, Boulder, CO, 1997.
[9] R. D. Martinez and R. C. Compton, "A general approach for the *s*-parameter design of oscillators with 1- and 2-port active devices," *IEEE Trans. Microwave Theory Tech.*, vol. 40, pp. 569–574, Mar. 1992.
[10] E. Yablonovitch, "Photonic band-gap structures," *J. Opt. Soc. Amer. B*, vol. 10, pp. 283–294, Feb. 1993.
[11] J. D. Joannopoulos, R. D. Meade, and J. N. Winn, Eds., *Photonic Crystals: Molding the Flow of Light*. Princeton, NJ: Princeton Univ. Press, 1995, ch. 4, pp. 740–747.
[12] T. Mader, S. Bundy, and Z. B. Popović, "Quasi-optical VCO's," *IEEE Trans. Microwave Theory Tech.*, vol. 41, pp. 1775–1781, Oct. 1993.

Qi Sun (S'97) was born in China in October 1961. She received the B.S. degree in electronic physics from Nanjin University, Nanjin, China, in 1983, and the M.S. degree in electrical engineering from the University of Hawaii at Manoa in 1998.

From 1983 to 1994, she was an electrical engineer at Nanjin Research Institute of Electronic Technology, China, developing active microwave circuits and receiver systems. She is currently a Senior Staff Engineer at Hughes Space and Communications, El Segundo, CA, working on satellite payload subsystems.

Jason B. Horiuchi was born in Seoul, Korea, in 1975. He is currently working toward the B.S. degree in electrical engineering at the University of Hawaii at Manoa.

In the summer of 1998 he was an intern at Raytheon Systems Company in the Solid-State Microwave Department, where he worked on switches and filters for airborne radar systems.

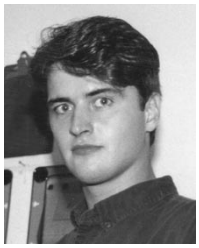

Steven R. Haynes (S'96) was born in Elkton, MD, on June 2, 1971. He is currently working toward the B.S. degree in electrical engineering at the University of Hawaii at Manoa.

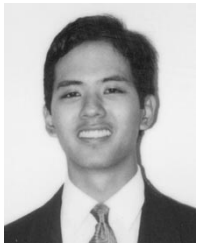

Kevin W. Miyashiro (S'96) was born in Honolulu, HI in 1975. He received the B.S. degree in electrical engineering from the University of Hawaii at Manoa in 1997.

He served as a Research Assistant from 1997 to 1998 at the University of Hawaii at Manoa. He served as Vice-President for Eta Kappu Nu, and was named Student Engineer of the Year in 1998. Currently, he is a Member of the Technical Staff at Raytheon Systems' Solid-State Microwave Center, where he works on GaAs MMIC's for transmit and receive modules.

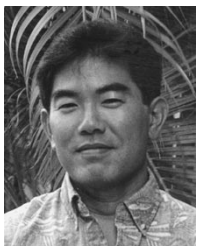

Wayne A. Shiroma (S'85–M'96) received the B.S. degree from the University of Hawaii at Manoa in 1986, the M.Eng. degree from Cornell University, Ithaca, NY, in 1987, and the Ph.D. degree from the University of Colorado at Boulder in 1996, all in electrical engineering.

In 1996, he joined the University of Hawaii at Manoa as an Assistant Professor of Electrical Engineering. He also served as a Member of the Technical Staff at Hughes Space and Communications, El Segundo, CA, developing solid-state power amplifiers for satellite communications. His research interests include microwave and millimeter-wave integrated circuits and antennas.